

AD-A231 958

## REPORT DOCUMENTATION PAGE

1a. REPORT SECURITY CLASSIFICATION			1b. RESTRICTIVE MARKINGS		
2a. SECURITY CLASSIFICATION AUTHORITY			3. DISTRIBUTION / AVAILABILITY OF REPORT		
2b. DECLASSIFICATION / DOWNGRADING SCHEDULE			Approved for public release; distribution unlimited		
4. PERFORMING ORGANIZATION REPORT NUMBER(S) Technical Report No. 1			5. MONITORING ORGANIZATION REPORT NUMBER(S)		
6a. NAME OF PERFORMING ORGANIZATION MIT, Dept. of Chem. Eng.		6b. OFFICE SYMBOL (If applicable)	7a. NAME OF MONITORING ORGANIZATION Office of Naval Research		
6c. ADDRESS (City, State, and ZIP Code) MIT Building 66, Room 554 Cambridge, MA 02139			7b. ADDRESS (City, State, and ZIP Code) 800 N. Quincy Street Arlington, VA 22217		
8a. NAME OF FUNDING / SPONSORING ORGANIZATION ONR		8b. OFFICE SYMBOL (If applicable)	9. PROCUREMENT INSTRUMENT IDENTIFICATION NUMBER N00014-91-J-1045		
8c. ADDRESS (City, State, and ZIP Code) 800 N. Quincy Street Arlington, VA 22217			10. SOURCE OF FUNDING NUMBERS		
			PROGRAM ELEMENT NO.	PROJECT NO. 4132047	TASK NO. 02
			WORK UNIT ACCESSION NO. 1		
11. TITLE (Include Security Classification) Evaluation of Domain Spacing Scaling Laws for Semicrystalline Diblock Copolymers					
12. PERSONAL AUTHOR(S) K.C. Douzinas, R.E. Cohen, A.F. Halasa					
13a. TYPE OF REPORT Technical Report		13b. TIME COVERED FROM _____ TO _____		14. DATE OF REPORT (Year, Month, Day) January 28, 1991	
				15. PAGE COUNT 15	
16. SUPPLEMENTARY NOTATION					
17. COSATI CODES			18. SUBJECT TERMS (Continue on reverse if necessary and identify by block number)		
FIELD	GROUP	SUB-GROUP	semicrystalline block copolymers		
			morphology		
			microphase separation theories		
19. ABSTRACT (Continue on reverse if necessary and identify by block number) Diblock copolymers of (ethylene-co-butylene)-b-(ethylethylene) (EBEE) were used to evaluate scaling laws describing the molecular weight dependence of the lamellar domain spacing of semi-crystalline block copolymer systems. Small angle X-ray scattering was used to measure lamellar domain spacings for a series of EBEE samples. Experimental results were in good agreement with the predictions of the equilibrium theory of Whitmore and Noolandi.					
20. DISTRIBUTION / AVAILABILITY OF ABSTRACT <input checked="" type="checkbox"/> UNCLASSIFIED/UNLIMITED <input type="checkbox"/> SAME AS RPT. <input type="checkbox"/> DTIC USERS			21. ABSTRACT SECURITY CLASSIFICATION unclassified		
22a. NAME OF RESPONSIBLE INDIVIDUAL			22b. TELEPHONE (Include Area Code)		22c. OFFICE SYMBOL

OFFICE OF NAVAL RESEARCH  
Contract N00014-91-J-1045  
R&T Code 4132047---02-1

TECHNICAL REPORT NO. 1

Evaluation of Domain Spacing Scaling Laws for Semicrystalline Diblock Copolymers

by

K.C. Douzinas and R.E. Cohen  
Department of Chemical Engineering  
Massachusetts Institute of Technology  
Cambridge, MA 02139

A.F. Halasa  
Goodyear Tire and Rubber Company  
Akron, OH 44305-0001

January 28, 1991

Accession For	
NTIS GRA&I	<input checked="checked" type="checkbox"/>
DTIC TAB	<input type="checkbox"/>
Unannounced	<input type="checkbox"/>
Justification	
By	
Distribution/	
Availability Codes	
Dist	Avail and/or Special
A-1	



Reproduction in whole or in part is permitted for any purpose of the U.S. government.

This document has been approved for public release and sale; its distribution is unlimited.

# **Evaluation of Domain Spacing Scaling Laws for Semi-crystalline Diblock Copolymers.**

Konstadinos C. Douzinas and Robert E. Cohen\*

Department of Chemical Engineering, Massachusetts Institute of Technology, 77 Massachusetts Ave., Cambridge, MA. 02139.

Adel F. Halasa

Goodyear Tire and Rubber Co, Research Division,  
142 Goodyear Blvd., Akron, OH. 44305-0001.

**ABSTRACT:** Diblock copolymers of (ethylene-co-butylene)-b-(ethylethylene) (EBEE) were used to evaluate scaling laws describing the molecular weight dependence of the lamellar domain spacing of semi-crystalline block copolymer systems. Small angle X-ray scattering was used to measure lamellar domain spacings for a series of EBEE samples. Experimental results were in good agreement with the predictions of the equilibrium theory of Whitmore and Noolandi.

## **Introduction.**

The molecular weight dependence of lamellar microdomain spacings of amorphous microphase separated block copolymer systems has been extensively studied [1-5]. Existing theories use

various approaches to arrive at a power law expression:

$$D \propto Z_t^{2/3} \quad (1)$$

where  $Z_t$  is the total degree of polymerization of the amorphous diblock. Experimental verification of this power law has been attempted using (styrene)-b-(isoprene) [6,7] and (styrene)-b-(2vinylpyridine) [8] diblock copolymers. These studies have shown that the 2/3 exponent accurately represents the domain spacing behavior. This validates the use of Gaussian chain modelling for amorphous blocks in confined microdomains.

In the case of semi-crystalline diblock copolymers however, the theoretical description of the equilibrium state becomes more complicated since the possibility of crystallization of one of the blocks must be taken into account. An equilibrium theory has been proposed by Whitmore and Noolandi [9], using a chain-folding model for the crystallizable block, a Gaussian chain model for the amorphous block and localization of the chemical junction which connects the two blocks in a narrow interface. The power law which describes the behavior of the lamellar long period is:

$$D \propto Z_t * Z_a^{-5/12} \quad (2)$$

where  $Z_t$  is the total degree of polymerization and  $Z_a$  is the degree of polymerization of the amorphous block. DiMarzio et al. [10] developed a similar power law with a different exponent for the amorphous block contribution:

$$D \propto Z_t * Z_a^{-1/3} \quad (3)$$

These theories have not been critically tested yet. As has been shown for (styrene)-b-(ethylene-co-butylene) (SEB) copolymers [11], the processing history used in sample

preparation is critical in determining whether a kinetically locked or equilibrium morphology is achieved. Past studies of (styrene)-b-(ethylene oxide) [12-16], (styrene)-b-( $\epsilon$ -caprolactone) [17,18] and (butadiene)-b-(ethylene oxide) [19] semi-crystalline diblocks have not addressed this matter in detail. In this work we attempt to evaluate the scaling law using a model system of (ethylene-co-butylene)-b-(ethylethylene) (EBEE). EBEE is well suited to this purpose because it fulfills the requirements of the theory: EBEE has a very narrow molecular weight distribution, the crystallization behavior of the ethylene-co-butylene block is thoroughly understood [20] and EBEE can be easily processed to give films with the necessary equilibrium morphology.

#### Experimental Section.

EBEE diblock copolymer samples were prepared by catalytic hydrogenation of precursor diblocks of 1,4-polybutadiene-b-1,2-polybutadiene (4B2B) which were polymerized anionically. The 1,4 PB blocks contained 45% cis-1,4, 45% trans-1,4 and 10% vinyl repeat units. The 1,2 PB blocks were 99% atactic 1,2. Transmission electron microscopy was carried out on several of these precursor copolymers using staining procedures described earlier [21]. A typical result is shown in Figure 1. The catalytic hydrogenation procedure is described in detail elsewhere [11,22]. It is important to note that we have carefully verified that the hydrogenation of the 4B2B diblocks is complete and that there is no degradation, chain scission or

chain coupling of the 4B2B precursor molecules. The molecular weights of the 4B2B samples were measured using GPC complemented by  $H^1$ -NMR; the corresponding molecular weights of EBEE were calculated using the stoichiometry of the hydrogenation reaction. These molecular weights are listed in Table I. EBEE films were prepared by spincoating [23] from 5wt% xylene solutions at 95°C. The films were subsequently dried under vacuum.

SAXS measurements were performed at room temperature using a Rigaku rotating Cu anode X-ray source ( $\lambda=1.54\text{\AA}$ ) with a Charles Supper double mirror focussing system and a Nicolet 2D area detector. The sample to detector distance was varied between 220 and 245cm and a helium filled beamline tube was used to reduce background scattering. Scattering measurements were performed using three sample orientations with the X-ray beam parallel to the X, Y and Z axes as shown in Figure 2. The scattered intensities were corrected for sample absorption and detector inhomogeneities.

## Results

A sample set of 2D scattered intensity patterns are shown in Figure 3. The corresponding intensity ( $I(Q)$ ) vs scattering vector magnitude ( $Q$ ) plot for irradiation parallel to the X-axis is shown in Figure 4, where  $Q=(4\pi/\lambda)\sin\theta$  and the scattering angle is  $2\theta$ . Arcs are observed in the 2D pattern when the samples are irradiated parallel to the X and Y axis, while there is no significant scattering when the samples are irradiated parallel to the Z axis. This information indicates that the lamellae are

predominantly parallel to the XY plane, but their orientation is not perfect. The lamellar domain spacing, or long period D, is calculated from these data using Bragg's diffraction law:

$D = 2\pi n/Q_p$ , where  $Q_p$  is the magnitude of the scattering vector at the intensity peak position and  $n$  is the peak order. In all our samples we observed only primary peaks, i.e.  $n=1$ . Values for the lamellar domain spacing of our samples are shown in Table II.

### Discussion

Plots to examine the two scaling laws are shown in Figures 5 and 6. Both theories seem to adequately predict the general trend of the data within experimental error. Although it is difficult to differentiate between the two theoretical models, due to resolution limitations of SAXS measurements of D-spacings, to test the validity of Eqs. 2 and 3, we have plotted  $\ln(D/Z_c)$  versus  $\ln(Z_s)$  in Figure 7. The theories predict straight lines with slopes of  $-5/12$  (Noolandi) and  $-1/3$  (DiMarzio). Such lines are shown in Figure 7 only for slope comparison and their position on the vertical axis has been arbitrarily chosen to clearly illustrate the relationship between predicted and experimental slopes. The least squares best fit to the experimental data for the EBEE samples gives a line with a slope of  $-0.42$ , which, for practical purposes, is indistinguishable from  $-5/12$ . We conclude that Noolandi's theory achieves a slightly better prediction of the scaling behavior of the lamellar long period in semi-crystalline diblock copolymers.

It is extremely interesting to note that some of the semi-

crystalline EBEE block copolymer samples with significantly different molecular weights display almost identical lamellar spacings, while their amorphous counterparts always exhibited larger spacings with increased molecular weight as predicted by Eq. 1. The different behavior of the semi-crystalline diblocks can be understood by taking into account the degree of chain folding in the EB block [9]. The equilibrium degree of chain folding is affected by the transverse dimensions of the flexible amorphous chain. If the molecular weight of the crystalline block remains constant and the molecular weight of the amorphous block increases, the crystalline chain will have to fold more to accomodate the increase in the transverse dimensions of the amorphous chain. This increased amount of folding leads to a corresponding decrease in the thickness of the crystalline lamellae. It is therefore possible for increases in the thickness of the amorphous lamellae to be counterbalanced by decreases in the thickness of the crystalline lamellae; thus the lamellar long period may remain virtually unaffected despite the change in block molecular weights.

The actual orientation of the chain-folded molecules with respect to the lamellar microdomain structure is also of great interest. According to Noolandi's model the chain axis of the EB blocks should be essentially normal to the plane of the lamellae. In other words the EB chains should be parallel to the Z-axis. Experimental examination of this prediction is currently being carried out on EBEE samples using wide angle X-ray diffraction pole figure analysis.



Aknowledgements: This research was supported by the Office of Naval Research, the Goodyear Tire and Rubber Company and by the Bayer Professorship in Chemical Engineering at M.I.T.

## REFERENCES:

1. Meier, D.J., Block and Graft Copolymers; Burke, J.J.; Weiss, V., Eds., Syracuse University Press, Syracuse, N.Y. 1973.
2. Meier, D.J., Polym. Prepr. (Am. Chem. Soc., Div. Polym. Chem.) 1974,15,171.
3. Helfand, E., Macromolecules, 1975,8,552.
4. Helfand, E.; Wasserman, Z.R., Macromolecules, 1976,9,879.
5. Helfand, E.; Wasserman, Z.R., Macromolecules, 1978,11,960.
6. Hashimoto, T.; Shibayama, M.; Kawai, H., Macromolecules, 1980,13,1237.
7. Hadziioannou, G.; Skoulios, A., Macromolecules, 1982,15,258.
8. Matsushita, Y.; Mori, K.; Saguchi, R.; Nakao, Y.; Noda, I. and Nagasawa, M., Macromolecules, 1990,23,4313.
9. Whitmore, M.D.; Noolandi, J., Macromolecules, 1988,21,1482.
10. DiMarzio, E.A.; Guttman, C.M.; Hoffman, J.D., Macromolecules, 1980,13,1194.
11. Cohen, R.E.; Cheng, P.-L.; Douzinas, K.; Kofinas, P.; Berney, C.V., Macromolecules, 1990,23,324.
12. Lotz, B.; Kovacs, A.J., Kolloid Z. & Z. fur Polym., 1966,209 97.
13. Lotz, B.; Kovacs, A.J.; Bassett, G.A.; Keller, A., Kolloid Z. & Z. fur Polym., 1966,209,115.
14. Gervais, M.; Gallot, B., Makromol. Chem., 171, 157(1973).
15. Gervais, M.; Gallot, B., Makromol. Chem., 174, 193(1973).
16. Gervais, M.; Gallot, B., Makromol. Chem., 178, 2071(1977).

17. Herman, J.-J.; Jerome, R.; Teyssie, P.; Gervais, M.; Gallot, B., Makromol. Chem., 179, 1111(1978).
18. Gervais, M.; Gallot, B., Makromol. Chem., 182, 997(1981).
19. Gervais, M.; Gallot, B., Makromol. Chem., 178, 1577(1978).
20. Howard, P.R.; Crist, B., Journal of Polym. Sci., Part B Polym. Phys., Vol. 27, 2269(1989).
21. Cohen, R.E.; Wilfong, D.E., Macromolecules, 1982,15,370.
22. Halasa, A.F. U.S. Patent 3 872 072.
23. Bates, F.S.; Cohen, R.E.; Argon, A.S., Macromolecules, 1983,16,1108.

## LIST OF TABLES AND FIGURES.

Table I. Molecular Weight Characterization of EBEE.

Table II. Comparison of Experimental Lamellar long periods with Theoretical Predictions.

Figure 1. TEM micrograph of 4B2B precursor for EBEE-144(62/72).

Figure 2. Sample and Microstructure orientation for SAXS experiments.

Figure 3. 2D SAXS patterns for EBEE-144(62/72).

Figure 4. Average Scattered intensity for EBEE-144 along the X-axis.

Figure 5. Noolandi Scaling Law.

Figure 6. DiMarzio Scaling Law.

Figure 7. Comparison of Noolandi and DiMarzio Scaling Laws (Theoretical lines are displayed for slope comparison only).

**TABLE I.****Molecular Weight Characterization of EBEE.**

<b>SAMPLE</b>	<b>M<sub>n</sub>*10<sup>-3</sup> (GPC-NMR)</b>	<b>M<sub>w</sub> / M<sub>n</sub> (GPC)</b>
<b>EBEE-1</b>	<b>60/7</b>	<b>1.09</b>
<b>EBEE-2</b>	<b>36/6</b>	<b>1.03</b>
<b>EBEE-3</b>	<b>19/3</b>	<b>1.07</b>
<b>EBEE-136</b>	<b>82/76</b>	<b>1.20</b>
<b>EBEE-138</b>	<b>35/53</b>	<b>1.14</b>
<b>EBEE-140</b>	<b>81/35</b>	<b>1.11</b>
<b>EBEE-142</b>	<b>52/89</b>	<b>1.10</b>
<b>EBEE-144</b>	<b>62/72</b>	<b>1.11</b>
<b>EBEE-146</b>	<b>91/71</b>	<b>1.18</b>
<b>EBEE-148</b>	<b>124/63</b>	<b>1.12</b>

**TABLE II.**

**Comparison of Experimental Lamellar long-periods with  
Theoretical Predictions.**

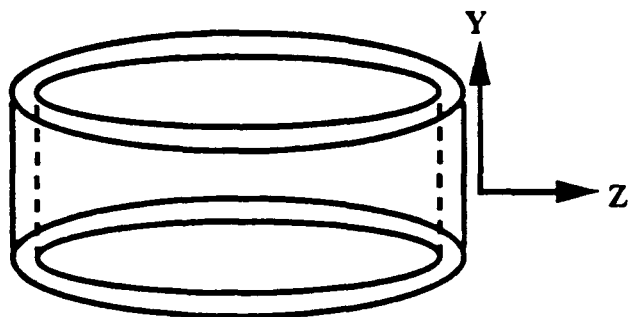
<b>SAMPLE</b>	<b>Mn*10<sup>-3</sup></b>	<b>Zt</b>	<b>Za</b>	<b>D(Å)</b> Noolandi	<b>D(Å)</b> DiMarzio	<b>D(Å)</b> Measured
EBEE-1	60/7	1204	130	720	590	680
EBEE-2	36/6	759	111	480	390	520
EBEE-3	19/3	389	56	330	250	* <sup>1.</sup>
EBEE-136	82/76	2815	1352	630	640	650
EBEE-138	35/53	1574	944	410	400	460
EBEE-140	81/35	2074	629	640	600	680
EBEE-142	52/89	2519	1593	530	540	520
EBEE-144	62/72	2389	1278	550	550	550 <sup>2.</sup>
EBEE-146	91/71	2889	1259	670	670	650
EBEE-148	124/63	3352	1130	810	800	* <sup>3.</sup>

- NOTES: 1. Sample EBEE-3 was homogeneous and had virtually no crystallinity.  
2. The D-spacing of EBEE-144 was used as a convergence point for comparing the slopes of theoretically predicted and experimentally measured scaling laws.  
3. The D-spacing of sample EBEE-148 was too large to be measured with the existing SAXS setup.

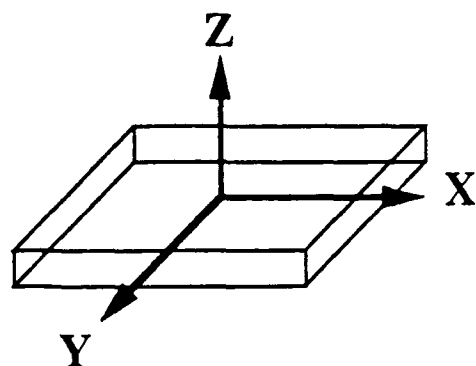
FIGURE 1.



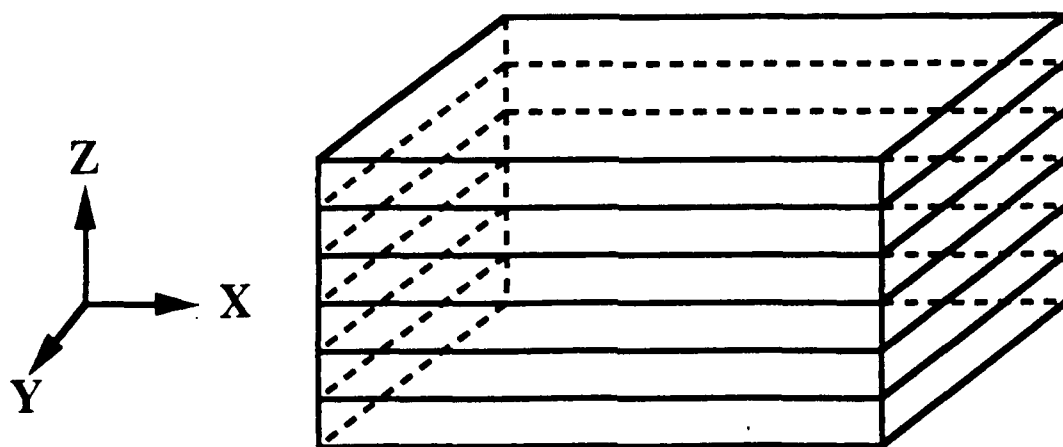
**FIGURE 2.**



**A. Spincast Film**



**B. SAXS Sample**



**C. Proposed Lamellar Structure.**



**FIGURE 3.**

**TWO DIMENSIONAL SCATTERING PATTERNS  
FOR SAMPLE EBEE-144 (62/72).**

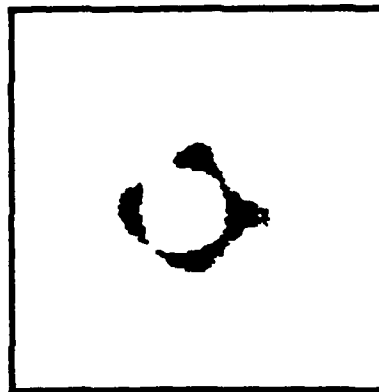
**X-AXIS**



**Y-AXIS**



**Z-AXIS**



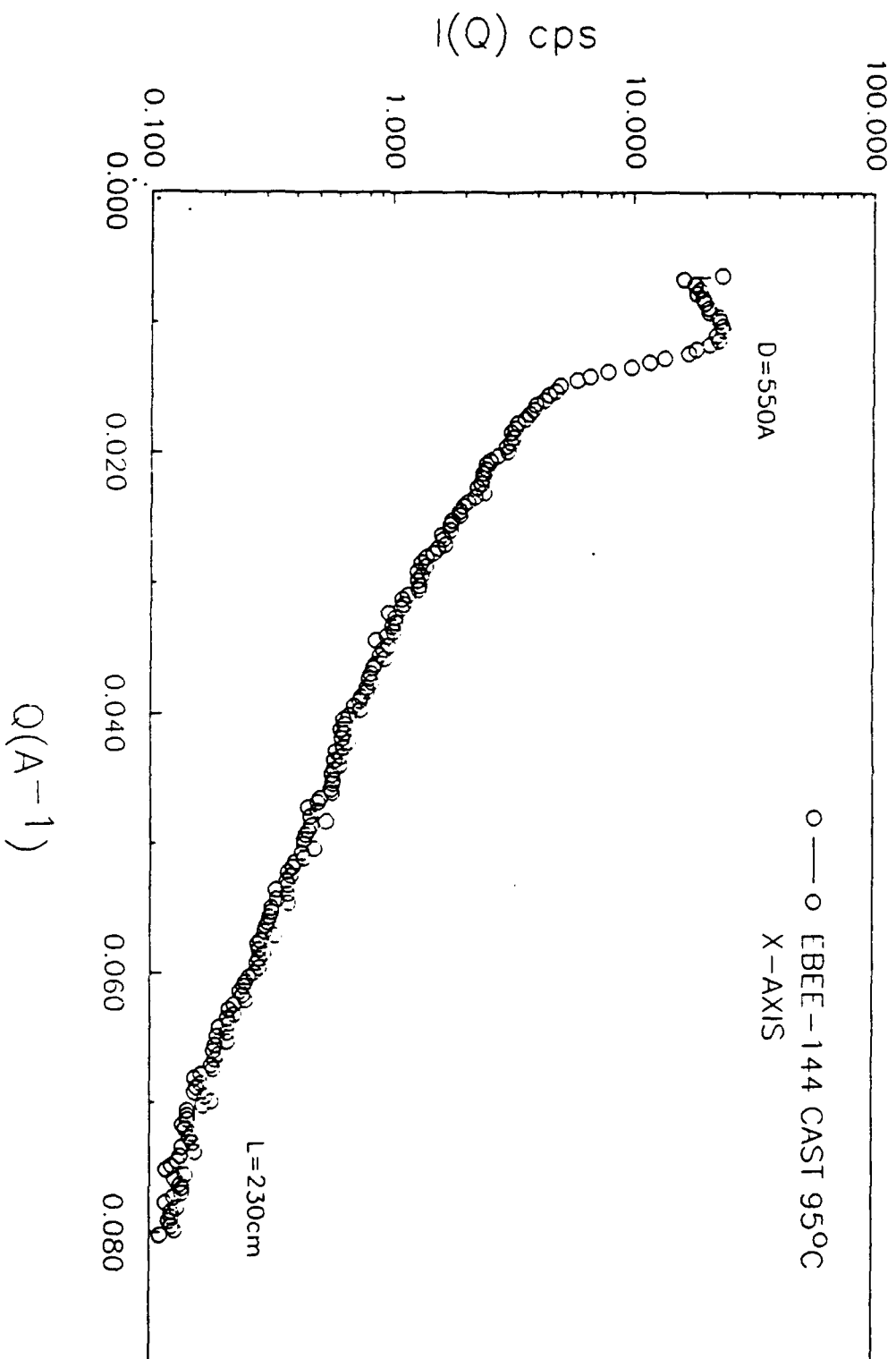


Figure 4.

Figure 5.

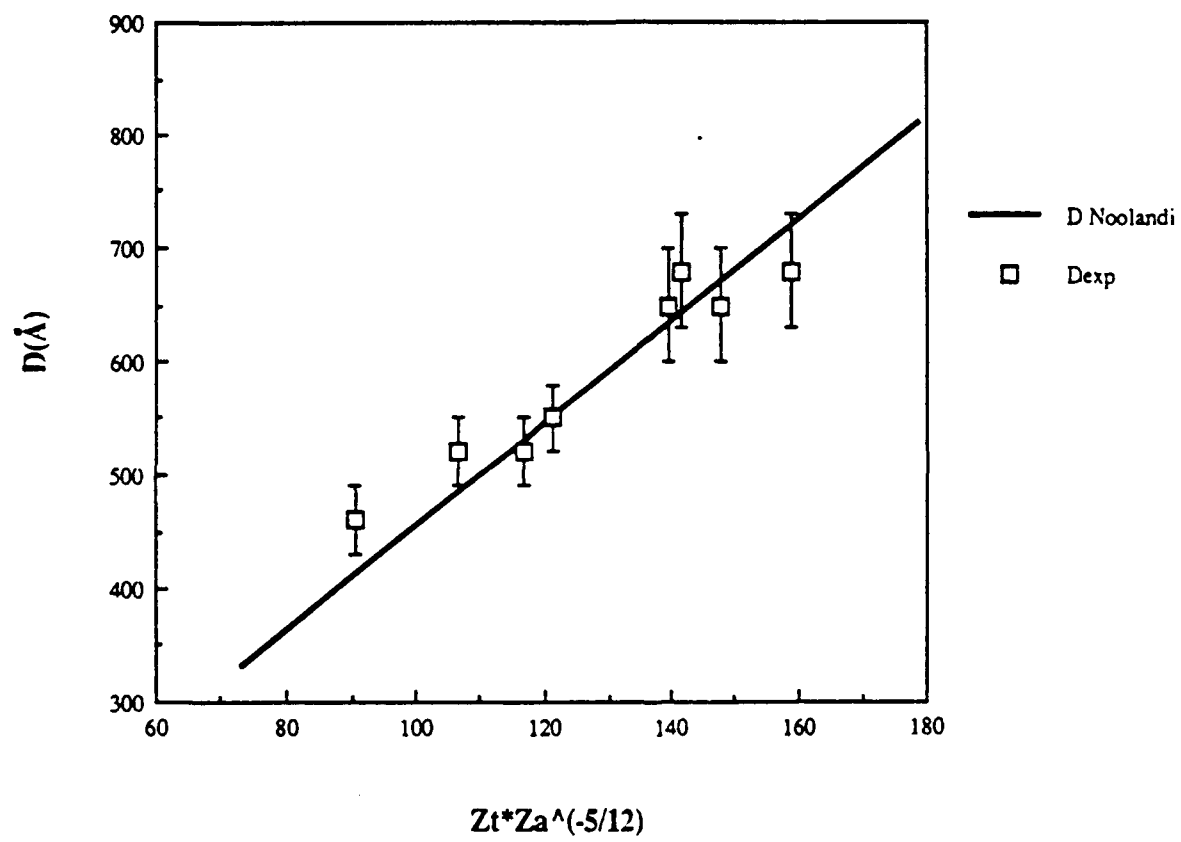


Figure 6.

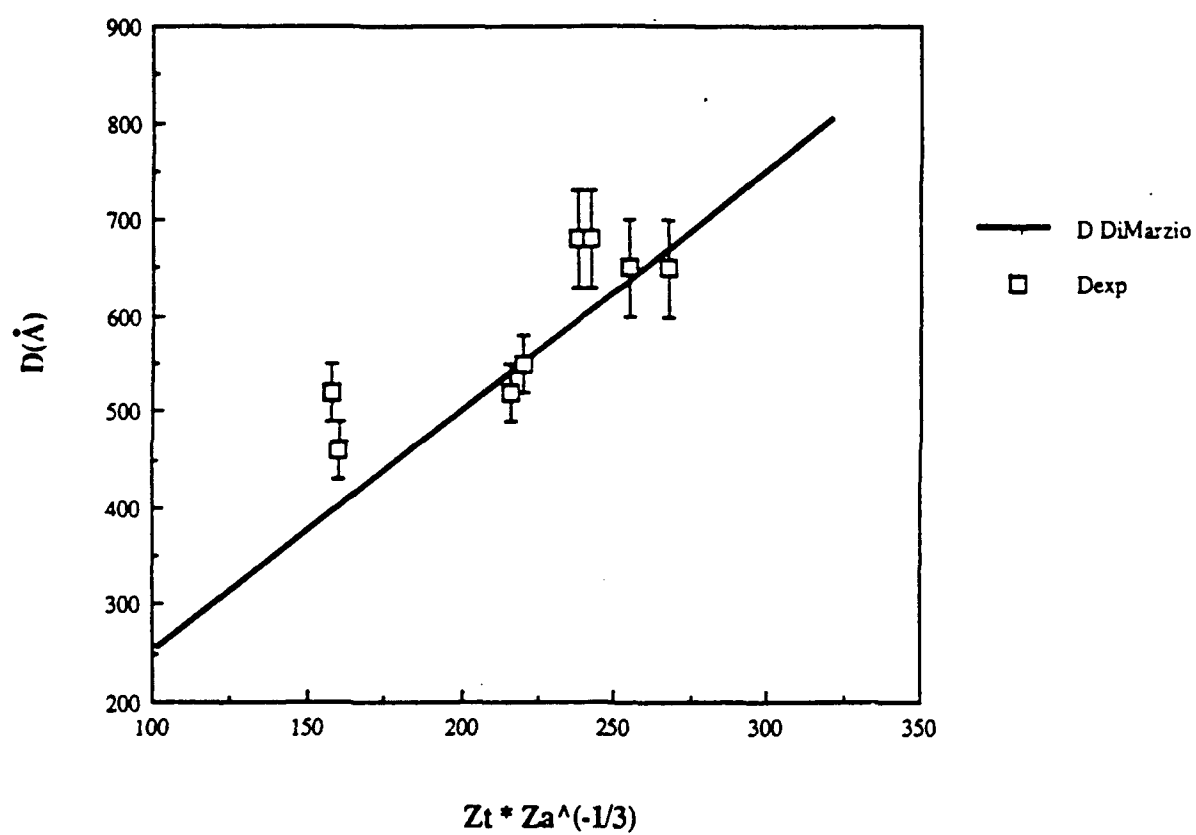


Figure 7.

